Prepared in Cooperation with
THE STATE OF CONNECTICUT
Geological and Natural History Survey

OPEN-FILE REPORT 03-487-A, v. 1.0
Plate 2 of 2
Explanatory pamphlet accompanies map

Brittle Structure Map

Structures on this map include joints, joints sets, faults, and parting fractures. Parting fractures are parallel to schistosity, layer parallel schistosity, axial surface of folds, cleavage, gneissosity, and bedding, and the same symbols used on Plate 1 are used here. Consult Plate 1 of this report for the Descriptionof Map Units and the Explanation of Map Symbols.

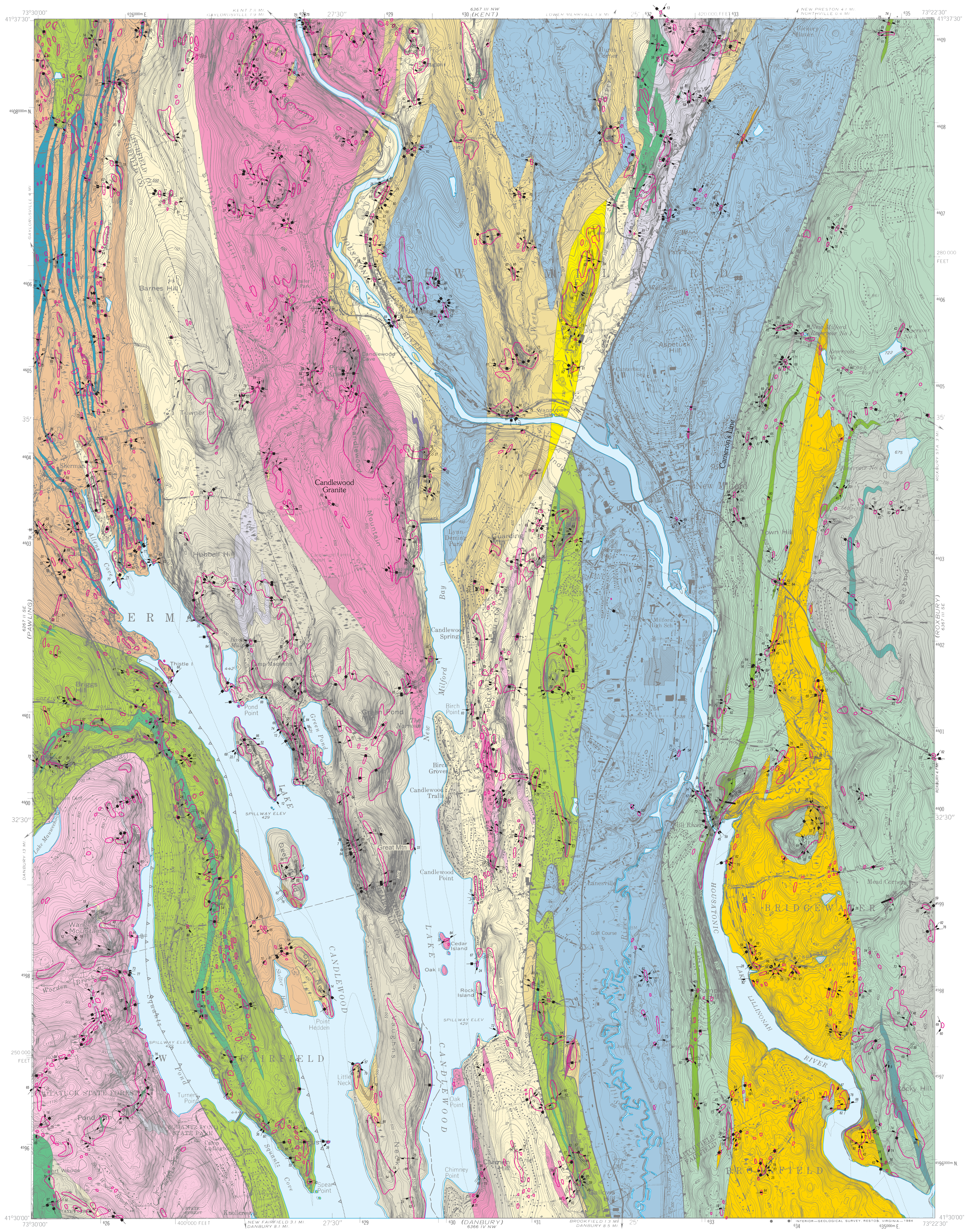

Base from U.S. Geological Survey, 1955
Photorevised 1984

Hydrography from Connecticut Map And Geographic Information Center (http://magic.lib.uconn.edu/)

Polyconic projection.
1927 North American Datum

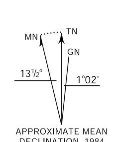

SCALE 1:24 000

CONTOUR INTERVAL 10 FEET
NATIONAL GEODETIC VERTICAL DATUM OF 1929

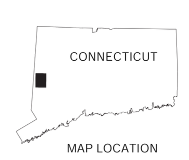

MAP LOCATION

Geology mapped by Walsh in 2000 and 2001. Geology digitized by Walsh, assisted by Lance Downing[2].

Map compiled from the digital bedrock database of the New Milford quadrangle. GIS database compiled in ARC/INFO version 8.1. Topography obtained by scanning a photo positive of the New Milford quadrangle at 400 dpi. Final cartography compiled in Adobe Illustrator version 8.0.

Domain 1 (n = 76)

#	%	Nor. H.	Azimuth	sd
1	33.7	100.0	280.7°	6.1°
2	18.1	46.2	315.0°	7.0°
3	16.9	38.9	6.5°	7.8°
4	12.1	34.6	82.9°	6.3°
5	7.7	26.8	299.8°	5.2°

Domain 2 (n = 114)

#	%	Nor. H.	Azimuth	sd
1	21.8	100.0	296.3°	5.3°
2	12.0	60.5	283.5°	4.8°
3	15.2	48.8	18.2°	7.6°
4	8.3	45.2	310.9°	4.5°
5	15.2	48.3	83.1°	7.6°
6	5.0	24.2	1.1°	5.0°
7	6.9	33.2	327.0°	5.1°
8	9.2	31.8	49.4°	7.0°

Domain 3 (n = 114)

#	%	Nor. H.	Azimuth	sd
1	16.7	100.0	272.1°	4.9°
2	17.2	91.7	299.1°	5.5°
3	12.2	65.7	284.2°	5.4°
4	14.1	63.4	21.0°	6.5°
5	11.5	48.7	325.3°	6.9°
6	4.6	37.3	310.1°	3.6°
7	6.1	37.1	76.1°	4.8°
8	7.0	28.3	355.1°	7.2°

Domain 4 (n = 76)

#	%	Nor. H.	Azimuth	sd
1	50.9	100.0	287.2°	7.4°
2	14.4	33.0	311.6°	6.3°
3	18.0	29.4	9.1°	8.9°
4	9.1	16.9	295.2°	7.8°

Domain 5 (n = 22)

#	%	Nor. H.	Azimuth	sd
1	24.4	100.0	84.3°	5.9°
2	13.4	72.0	287.8°	4.5°
3	13.5	78.8	29.5°	4.2°
4	14.9	80.7	312.2°	4.5°
5	10.4	44.5	71.2°	5.7°
6	4.6	31.3	358.0°	3.6°
7	4.4	31.2	332.2°	3.5°
8	4.8	30.8	18.5°	3.8°
9	4.3	28.2	282.0°	3.7°
10	5.7	38.0	300.0°	3.6°

Domain 6 (n = 55)

#	%	Nor. H.	Azimuth	sd
1	19.2	100.0	318.2°	5.3°
2	14.6	63.5	289.1°	6.3°
3	14.5	67.6	19.5°	5.9°
4	16.7	61.0	272.9°	7.5°
5	7.6	54.3	344.8°	3.8°
6	7.4	48.8	5.0°	4.2°
7	6.1	44.7	309.0°	3.8°
8	4.3	30.6	327.0°	3.8°
9	6.4	24.0	56.1°	7.3°
10	3.4	19.2	299.7°	4.8°

Domain 7 (n = 108)

#	%	Nor. H.	Azimuth	sd
1	16.7	100.0	284.2°	5.3°
2	18.3	99.6	303.4°	5.8°
3	11.6	69.8	317.9°	5.2°
4	10.1	59.3	82.8°	5.3°
5	7.1	48.1	55.8°	4.7°
6	4.9	40.9	67.6°	3.7°
7	6.8	37.0	357.8°	5.8°
8	8.0	38.9	30.2°	6.5°
9	3.2	27.1	10.4°	3.7°

Domain 8 (n = 37)

#	%	Nor. H.	Azimuth	sd
1	42.6	100.0	292.3°	5.7°
2	13.1	33.0	85.6°	5.3°
3	14.1	22.6	6.5°	8.3°
4	11.3	29.8	333.3°	5.1°
5	6.7	28.3	314.5°	3.1°
6	13.3	10.6	75.5°	16.6°

Domain 9 (n = 40)

#	%	Nor. H.	Azimuth	sd
1	32.0	100.0	287.6°	5.4°
2	28.0	81.8	88.7°	5.8°
3	20.6	38.9	1.7°	8.9°
4	7.8	31.9	296.1°	4.1°
5	6.7	35.7	359.6°	3.2°

Domain 10 (n = 81)

#	%	Nor. H.	Azimuth	sd
1	16.3	93.2	43.8°	4.7°
2	17.4	87.5	87.8°	5.4°
3	18.1	100.0	61.9°	4.9°
4	17.4	61.4	343.6°	7.6°
5	8.2	33.9	280.2°	6.6°
6	4.8	31.0	77.5°	4.2°
7	8.5	20.5	300.1°	11.2°
8	3.6	25.0	51.3°	3.9°
9	5.9	19.3	29.2°	8.2°

Domain 11 (n = 86)

#	%	Nor. H.	Azimuth	sd
1	23.1	100.0	86.5°	5.6°
2	19.1	89.5	284.3°	5.1°
3	10.9	52.5	3.4°	5.0°
4	9.5	51.7	296.4°	4.4°
5	10.5	45.9	16.4°	5.5°
6	7.3	34.5	310.0°	5.1°
7	3.8	22.2	339.0°	4.2°
8	9.2	16.2	34.8°	13.7°
9	6.4	14.2	69.5°	10.8°

Domain 12 (n = 94)

#	%	Nor. H.	Azimuth	sd
1	15.7	100.0	68.0°	5.4°
2	13.3	83.4	47.8°	5.4°
3	8.2	66.8	282.9°	4.2°
4	7.9	62.2	270.6°	4.3°
5	9.0	46.2	33.7°	6.7°
6	6.2	46.8	306.3°	4.5°
7	4.9	34.9	290.3°	4.8°
8	4.2	38.1	77.5°	3.8°
9	3.0	28.8	58.9°	3.5°
10	4.8	17.5	346.3°	9.4°

Domain 13 (n = 68)

#	%	Nor. H.	Azimuth	sd
1	17.8	99.9	71.3°	6.3°
2	15.9	100.0	54.8°	5.6°
3	14.4	86.5	86.0°	5.9°
4	9.9	79.1	282.2°	4.4°
5	8.3	64.4	42.3°	4.5°
6	8.8	57.7	300.7°	5.4°
7	7.3	46.5	336.7°	5.5°
8	3.6	31.8	15.7°	4.0°
9	4.7	32.0	316.3°	5.2°
10	4.1	29.9	2.9°	4.9°

Domain 14 (n = 55)

#	%	Nor. H.	Azimuth	sd
1	33.9	100.0	83.2°	5.5°
2	13.4	44.4	58.1°	4.9°
3	14.3	34.4	277.8°	6.7°
4	7.5	31.7	345.0°	3.8°
5	17.4	27.7	37.0°	10.2°
6	13.4	19.3	304.1°	11.2°

Domain 15 (n = 80)

#	%	Nor. H.	Azimuth	sd
1	20.4	100.0	271.4°	5.6°
2	18.8	95.3	59.5°	5.4°
3	15.1	72.8	38.0°	5.7°
4	13.5	73.2	351.3°	5.0°
5	11.8	55.3	295.2°	5.8°
6	6.2	40.4	74.3°	4.2°
7	5.9	34.4	23.2°	4.7°
8	8.4	22.7	311.2°	10.1°

Domain 16 (n = 33)

#	%	Nor. H.	Azimuth	sd
1	19.3	100.0	285.5°	5.5°
2	18.2	91.5	79.6°	5.6°
3	13.1	64.8	46.2°	5.7°
4	10.1	64.0	31.2°	4.5°
5	8.5	41.3	272.1°	5.8°
6	7.9	45.5	321.7°	4.9°
7	8.6	42.1	300.1°	5.8°
8	7.4	39.7	57.4°	5.2°
9	4.0	29.9	19.0°	3.8°
10	3.1	23.4	6.0°	3.7°

Domain 17 (n = 87)

#	%	Nor. H.	Azimuth	sd
1	19.7	100.0	83.7°	5.8°
2	10.4	68.3	48.5°	4.5°
3	9.1	36.7	31.0°	7.4°
4	11.1	31.5	16.4°	10.4°
5	5.7	41.5	297.9°	4.1°
6	6.7	36.9	277.3°	5.4°
7	5.3	36.4	310.2°	4.3°

Table 1. Gaussian parameters for rose diagrams by domain.
n = number of data points
# = fracture trend number
% = percent data
Nor. H. = normalized height
Azimuth = azimuth of fracture trend
sd = 1 standard deviation of fracture trend.

Fracture Trend Analysis Map

This map shows lower hemisphere equal area projections (stereonets) and azimuth-frequency (rose) diagrams for steeply dipping (dip > 60°) fractures. The map is divided into 17 domains with north-south boundaries based on geologic contacts and east-west boundaries based on outcrop distribution (fig. 1). Analyzed data include brittle structures portrayed on the adjacent Brittle Structure Map. Stereonets include contoured poles to all fractures; contour interval is two percent. Rose diagrams show peaks identified by a Gaussian curve-fitting routine (Wise and others, 1985; Salvini and others, 1999) and peak parting-fracture trends. Table 1lists the Gaussian parameters for each domain. Figures 2 and 3 show the model results for the acute dihedral angle between the principal parting fracture trend and the principal jointing fracture trend. Data analysed with DAISY software version 3.41 (Salvini, 2002).

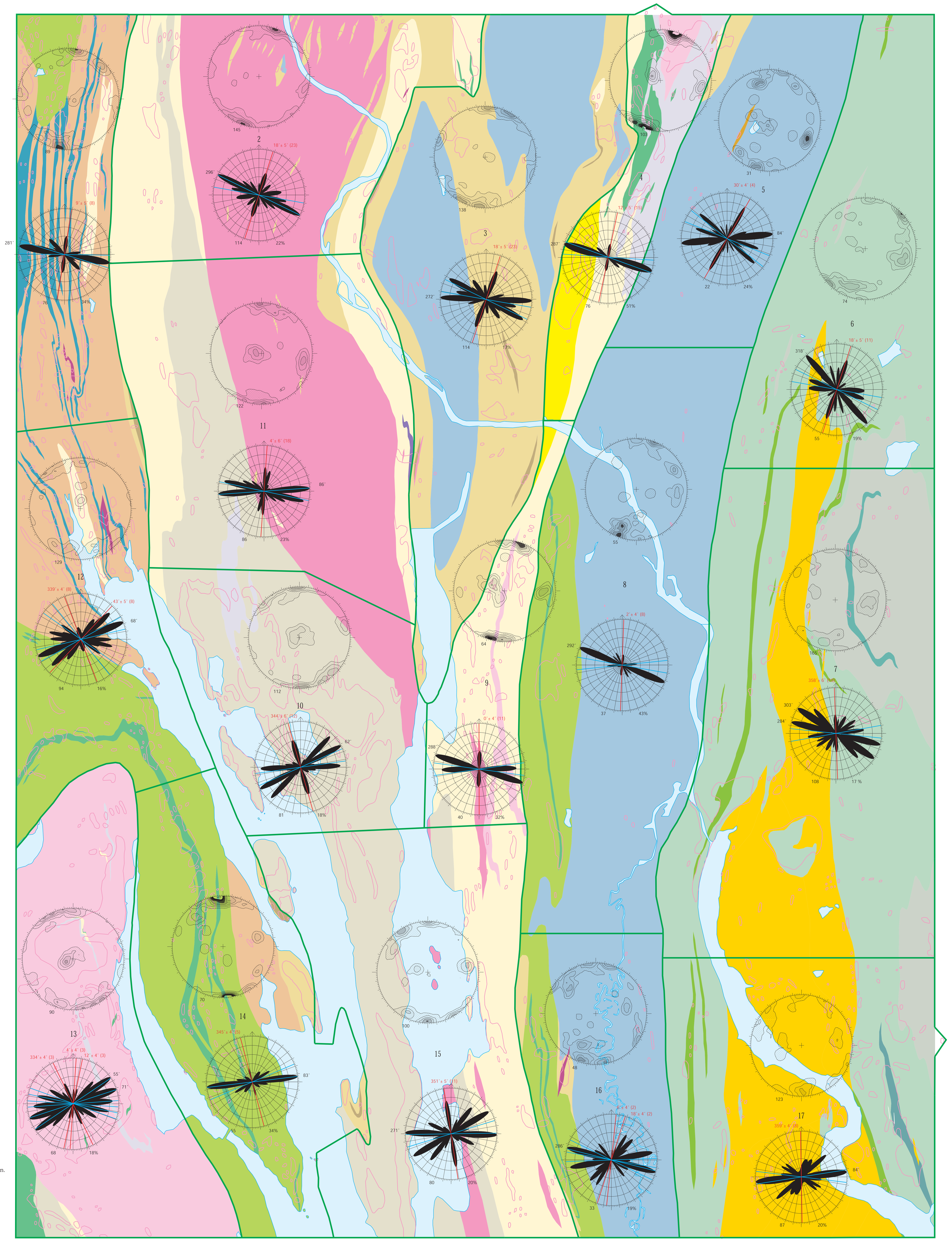

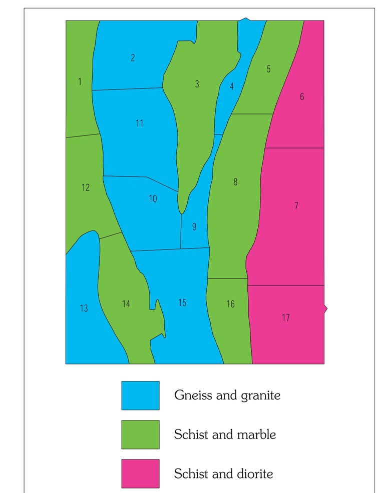

Figure 1. The fracture domains in this analysis are based on generalized geology. The north-south trending domain boundaries follow belts of similar rock types and the east-west trending boundaries are based on groups of closely spaced outcrops where fracture measurements were collected.

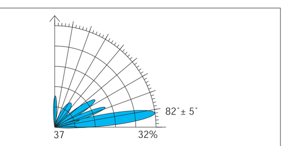

#	%	Nor. H.	Azimuth	sd
1	32.1	100.0	82.0°	4.7°
2	14.2	53.6	68.8°	3.9°
3	17.8	48.0	56.0°	5.4°
4	8.8	30.8	1.0°	4.2°
5	18.1	28.8	33.7°	9.1°
6	4.2	25.1	74.4°	2.5°
7	4.8	22.2	270.2°	3.1°

Figure 2. Rose diagram of the acute dihedral angle between parting fractures and all other fractures. The angle is calculated as the difference between the peak fracture trend for parting fractures and the principal fracture trends for each domain. Peak trends have a normalized height of 100 percent and principal trends have normalized heights of greater than 50 percent (Hardcastle, 1995). For example, the parting fracture trend for domain 2 is 18° (Fracture Trend Analysis Map), the peak fracture trend is 296°, and the remaining principal trend is 283° (Table 1, Plate 2). The acute dihedral angles for domain 2 are, therefore, 82° and 85°. See Table 1 for an explanation of the Gaussian parameters. The calculated peak acute dihedral angle of 82° demonstrates the orthogonal relationship between parting fractures and all other fractures in the area and closely matches the observed data (fig. 3.).

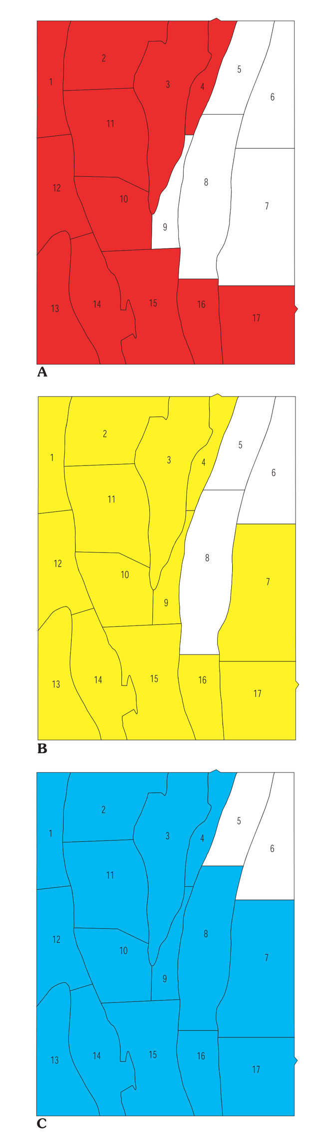

Figure 3. Maps showing results of comparison between the calculated peak acute dihedral angle (PADA = 82°) and fracture trends by domain. A) PADA agrees with peak trend within 1 sigma (± 5°) (red domains); B) PADA agrees with peak trend within 2 sigma (± 10°) (yellow domains); C) PADA agrees with peak trend within 3 sigma (± 15°) (blue domains). In the absence of comprehensive fracture data, the acute dihedral angle might be used for predicting regionally significant fracture trends in similar geologic settings where only foliation data are available.

Explanation of Fracture Trend Analysis Map Diagrams

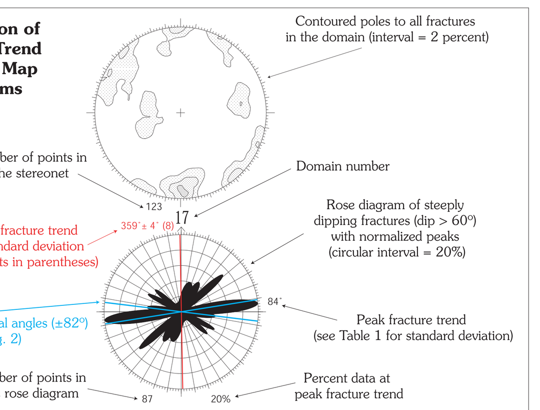

References Cited

Hardcastle, K.C., 1995, Photolineament factor: A new computer-aided method for remotely sensing the degree to which bedrock is fractured: Photogrammetric Engineering and Remote Sensing, v. 61, no. 6, p. 739-747.

Salvini, F., 2002, The Structural Data Integrated System Analyzer software (DAISY 3.28b), Dipartimento di Scienze Geologiche, Universita degli Studi di "Roma Tre", Rome, Italy.

Salvini, F., Billi, A., and Wise, D.U., 1999, Strike-slip fault propagation cleavage in carbonate rocks: the Mattinata Fault Zone, Southern Apennines, Italy: Journal of Structural Geology, v. 21, p. 1731-1749.

Wise, D. U., Funiciello, R., Parotto, M., and Salvini, F., 1985, Topographic lineament swarms: Clues to their origin from domain analysis of Italy: Geological Society of America Bulletin, v. 96, p. 952-967.

BEDROCK GEOLOGIC MAP OF THE NEW MILFORD QUADRANGLE, LITCHFIELD AND FAIRFIELD COUNTIES, CONNECTICUT

By
Gregory J. Walsh[1]
2003

AFFILIATIONS:
[1] U.S. Geological Survey
Montpelier, Vermont 05601
[2] Montpelier High School
Montpelier, Vermont 05601
[3] U.S. Geological Survey
East Hartford, Connecticut 06108

Plates 1 and 2 and the accompanying text are part A and the database is part B of this Open-File Report; both parts are available from: http://pubs.usgs.gov/of/2003/of03-487/

This map was produced on request, directly from digital files, on an electronic plotter.

For sale by U.S. Geological Survey, Map Distribution Box 25286, Federal Center, Denver, CO 80225
1-888-ASK-USGS